文章编号:1007 - 4252(2022)05 - 0005 - 433 DOI:10.20027/j.gncq.2022.0055

半导体型乙醇传感器研究近况

刘泽轩*,张甘英,吴 叶,范晓捷
(中国电子科技集团公司第五十八研究所,无锡 214035)

摘要:气体传感器在现代科学技术领域发挥着重要作用,它们被广泛用于公共安全、污染监测、呼吸分析、智能家居等。由于其低成本、高灵敏度、易制造的优势,促使众多研究人员对气体传感器展开广泛研究。尤其是金属氧化物半导体(MOS)型气体传感器,此类传感器可检测 150 多种有毒有害气体,对具有易挥发、易燃易爆性质的乙醇(C_2H_5OH)有机挥发性气体(VOCs)具有良好的气敏特性。本文回顾了近一年来最先进的 MOS 电阻型乙醇传感器,详细阐述了传感器对乙醇气体的传感机制;重点介绍了不同 MOS 型传感器对乙醇的敏感特性,分析了诸如金属掺杂、异质结复合材料以及 MOS 分等级结构对乙醇传感器性能的影响。通过分析可得,SnO_2、ZnO 基传感器对乙醇的传感性能最佳,特别是经金属掺杂和由不同导电类型半导体构建的异质结 MOS 传感器。

关键词:气体传感器;乙醇;传感性能
中图分类号:TP212; TQ134.32 **文献标志码**:A

Recent Research on Semiconductor-based Ethanol Sensors

LIU Ze-xuan*, ZHANG Gan-ying, WU Ye, FAN Xiao-jie
(China Electronics Technology Group Corporation NO. 58 Research Institute, Wuxi 214035, China)

Abstract: Gas sensors play an important role in modern science and technology; they are widely used in public safety, pollution monitoring, respiratory analysis, smart homes, etc. Their low cost, high sensitivity and ease of manufacture have prompted many researchers to conduct extensive research on gas sensors. In particular, metal oxide semiconductor (MOS) type gas sensors, which can detect more than 150 toxic and hazardous gases, have good gas-sensing properties for organic volatile gases (VOCs) such as ethanol (C_2H_5OH), which is volatile and flammable and explosive in nature. This paper reviews the state-of-the-art MOS resistive ethanol sensors in the last year and details the sensing mechanism of the sensors for ethanol gas; it highlights the sensitive characteristics of different MOS-based sensors for ethanol and analyses the effects of, for example, metal doping, heterojunction composites and MOS hierarchical structures on the performance of ethanol sensors. The analysis shows that SnO_2 and ZnO-based sensors have the best sensing performance to ethanol, especially MOS sensors doped with metals and constructed heterojunction from different conductive types of semiconductors.

收稿日期:2022-09-19; **修订日期**:2022-10-12
通信作者:刘泽轩(1995-),男,硕士,助理工程师,主要研究方向为气体传感器、集成电路版图设计(E-mail:liuzexuanlzx@163.com).

Key words: Gas Sensor; Ethanol; Sensing Performance

0 引言

近年来,在我国逐步推进生态环境朝着安全、健康发展的背景下,群众愈发关注日常生活及工作场所中空气质量对人体健康增添的潜在影响。较差的气氛环境极易对人身健康造成损害,尤其是在工业生产中,有机挥发性气体(Organic Volatile Gases, VOCs)易与空气混合引发爆炸等不确定性危害。有机挥发性气体包括乙醇、甲醇、苯、二甲苯等有机物所挥发出的气体,且该类气体在生产、贮藏、运输等环境中均存在安全隐患。譬如,在生产工业乙醇时,挥发出的高浓度乙醇气体易刺激人体上呼吸道黏膜,引发头痛、恶心等不良症状且易在高温环境中燃烧、爆炸。因此,做到实时监测乙醇气体浓度对防治上述安全隐患实属必要。

乙醇传感器能够有效检测气氛环境中乙醇气体浓度,保障空气质量符合标准,是一种将乙醇气体浓度模拟量以电信号的形式输出的信息采集器。自1931 年 Braver 发现氧化铜的电学性能随气体吸附而变化,到 1962 年 Seiyama 等人成功研制出可供检测氧气、一氧化碳等气体成分及浓度的气体传感器,至 1968 年 Taguchi 等人研发出可被商用的半导体型气体传感器[1],历经多年发展,乙醇气体传感器已更新迭代出多种基于不同工作原理的传感器类型,如:半导体型、接触燃烧型、光学型、电化学型等[2]。其中,半导体型传感器因其成本低、性能佳、制作便捷等优势被广泛应用于家庭、办公场所中。半导体型乙醇传感器通常由敏感元件、加热单元、电源线、信号线组成,敏感元件是由金属氧化物半导体(Metal Oxide Semiconductor, MOS)敏感材料构成,通过探测敏感材料电/化学性能变化以判别乙醇气体浓度。一般根据导电类型,敏感材料被分为 N 型氧化物和 P 型氧化物,常见的 N 型敏感材料有二氧化锡(SnO_2)[3]、氧化锌(ZnO)[4];常见的 P 型敏感材料有氧化镍(NiO)[5]、氧化铜(CuO)[6]。这些不同导电类型的敏感材料可经过差异化制程工艺制备出金属掺杂敏感材料和异质结敏感材料,以此方式达到改变敏感材料电、化学性能的目的,经改性后的敏感材料被用于敏感元件时也会有助于改善乙醇传感器性能或降低传感器功耗。半导体型乙醇传感器可按半导体自身物理特性分为电阻型和非电阻型[7]。电阻型是通过观测传感器在测量乙醇气体前后 MOS 阻值变化,进而分析得出乙醇浓度及干扰气体的一种器件类型;而非电阻型则是运用待测气体吸附或与 MOS 表面发生反应时产生的物理或化学特性间接得出乙醇气体相关信息的器件种类。如图 1 所示,图中显示了气体传感器的详细类别。虽然半导体型乙醇传感器类型多样,但主要影响传感器性能的是敏感材料对乙醇的气敏特性。

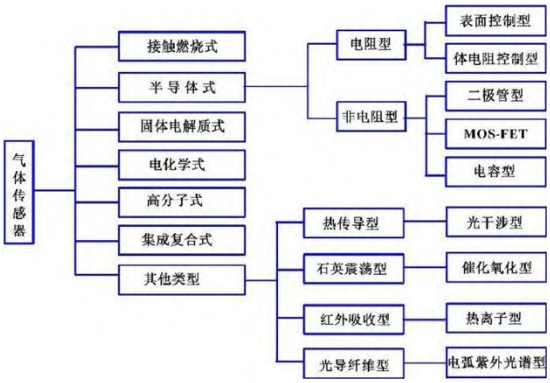

图 1 气体传感器分类

Fig. 1 Gas sensors classification

目前,纳米材料被普遍用作乙醇传感器敏感材料,常用水热法、微波水热法、溶剂热法、静电纺丝法等制备工艺合成 MOS 敏感材料[8-11]。水热法,起源于 19 世纪模拟成矿法,是指在密闭高压环境中,用水或水与乙醇混合液为溶剂,在高压高温环境中,利用温度差作用使反应物结晶成微/纳米材料。可通过改变反应物类型、前驱体液酸碱度、表面活性剂种类、反应时长及温度等要素生成具有分等级结构的敏感材料[12]。分等级纳米结构一般由零维纳米颗粒、一维纳米线、二维纳米片、三维纳米花等单元组成,如图 2 所示[13]。分等级结构单元,其比表面积、孔隙率、晶粒尺寸极大地影响传感器气敏性能,具有高比表面积、高孔隙率的敏感材料可以俘获更多乙醇气体分子利于 MOS 在气氛环境中电学性能变化,促使传感器气敏性能改善。

乙醇传感器的性能参数主要包括响应值(灵敏度)、响应/恢复时间、工作温度、检测限、选择性、稳定性[14]。响应值(灵敏度),表示传感器对乙醇气体

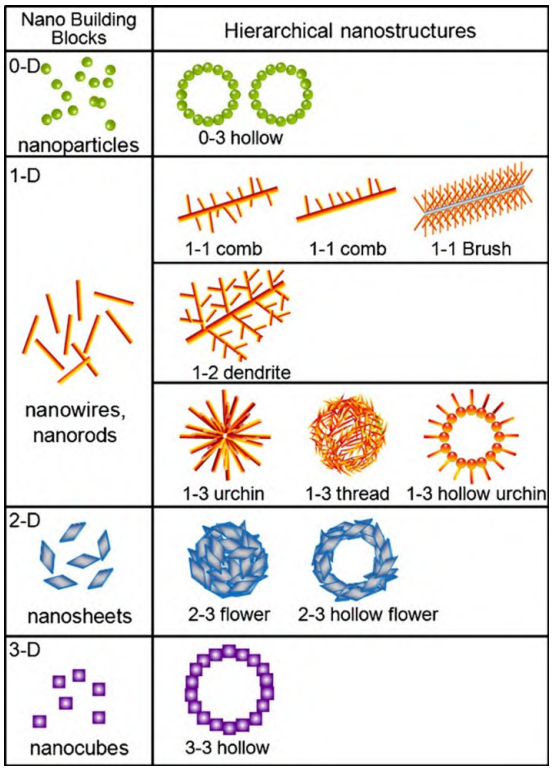

图 2　气体传感器分等级结构敏感材料[13]

Fig. 2 Sensing materials for gas sensor hierarchy [13]

的灵敏程度,大多被描述为传感器在测量乙醇气体前后阻值变化比,其被定义为 $S=R_g/R_a$(P 型乙醇传感器测量乙醇气体)或 $S=R_a/R_g$(N 型乙醇传感器测量乙醇气体),其中 R_a 为空气中的初始电阻,R_g 为待测目标物质气氛中的电阻;响应/恢复时间被描述为传感器遇乙醇气体前后阻值变化为总阻值 90% 所需要的时间;工作温度表示传感器处于最佳工作状态时的温度并与传感器功耗息息相关;检测限是指传感器可检测乙醇气体的浓度范围,一般来说检测限越低意味着传感器可以检测到环境中浓度更小的乙醇气体;选择性和稳定性一般描述传感器对乙醇气体的响应程度远高于干扰气体,在传感器使用期间其基线电阻漂移和响应值变化幅度较小。以上参数是设计高性能低功耗乙醇传感器的重要衡量标准。

本文主要研究了近一年来(2021 ~ 2022)基于金属氧化物半导体电阻型乙醇气体传感器[15-17]在环境监测上的发展及应用,总结了过去一年内传感器对乙醇气体的不同检测结果,并选择了部分性能优异、功耗较低的乙醇传感器进行分析。

1　乙醇传感器敏感机理

目前,国内外学者普遍认为表面吸附氧控制理论[18]是电阻型半导体式气体传感器的敏感原理。该原理是指被测气体分子与敏感材料上附着的电离化氧分子发生电荷交换,使半导体自身电阻率发生改变,进而演变成可测得传感器阻值变化的过程。在传感器发生敏化过程时,敏感材料表面通常会附着空气中游离的氧分子,这些氧分子在 100 ~ 500 ℃ 之间通过从半导体导带夺取电子,形成 O_2^-、O^-、O^{2-}[19],氧分子电离过程如下式所示:

$$O_2(\text{gas}) \rightarrow O_2(\text{absorbed}) \quad (1)$$

$$O_2(\text{absorbed}) + e^- \rightarrow O_2^-(\text{dissociative}) \quad (2)$$

$$O_2^-(\text{dissociative}) + e^- \rightarrow 2O^-(\text{dissociative}) \quad (3)$$

$$O^-(\text{dissociative}) + e^- \rightarrow O^{2-}(\text{dissociative}) \quad (4)$$

对于 N 型半导体,当传感器放在空气中时,半导体导带中电子与氧分子反应转化为氧阴离子,导致半导体阻值增大并在其晶粒表面形成电子耗尽层(Electron-Depletion Layer, EDL)[20];当被测气体接触传感器表面吸附氧后,被测气体与氧离子反应释放电子至半导体导带或更进一步夺取导带中电子,电子耗尽层宽度改变,使传感器阻值减小或增大。通常情况下,还原性气体在与氧离子反应时会释放可被半导体导带所能捕获的电子,促使半导体中电子数目激增,电导率增大;而具有氧化性的被测气体为达到能量最低原理,会继续捕获半导体导带中电子形成稳态分子,该过程会导致传感器阻值增大。而氧分子捕获 P 型半导体导带电子后,附着在半导体表面的氧离子会使半导体晶粒表面形成空穴积累层(Hole-Accumulation Layer, HAL)[21],当半导体表面接触还原性气体后,氧离子与被测气体反应所产生的电子会与空穴积累层中的空穴复合,致使以空穴为多数载流子的半导体导电性能降低。如图 3 所示,图中形象地表示出不同导电类型半导体在附着氧离子前后其晶粒表面形成的核-壳状导电区域[22]。

为更好表现传感器阻值变化原理,下式描述了半导体导电性能变化的本质原因:

$$\rho=\frac{1}{\sigma}=\frac{1}{nq\mu}$$

式中 ρ 为电阻率,σ 为电导率,n 为多数载流子数目,q 为电荷量,μ 为载流子迁移率。可以看出不论

是 N 型或是 P 型半导体,其电阻率与多数载流子数目呈负相关性。

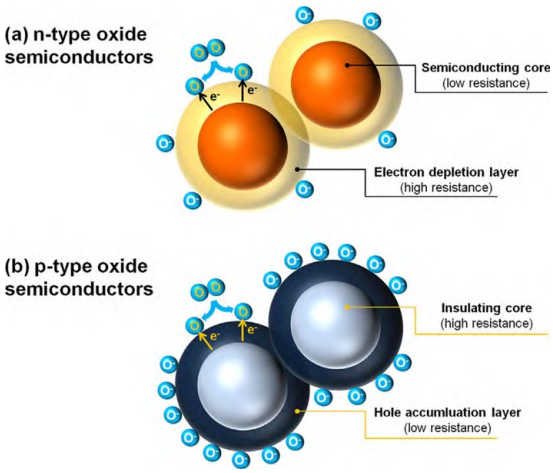

图 3 核—壳状导电区域(a)N 型半导体,(b)P 型半导体[22]

Fig. 3 Core-shell conducting regions (a) N-type semiconductor, (b) P-type semiconductor [22]

2 高性能乙醇传感器研究进展

近年来,传感器技术已持续发展并涉及到人类健康安全、空气质量以及环境保护等方面。文献调研中总结了大量不同氧化物半导体基乙醇传感器的特征及气敏性能,分析了各类氧化物半导体敏感材料的气敏特性。此类金属氧化物半导体(MOS)包括:ZnO、SnO_2、WO_3、CuO、In_2O_3、复合氧化物半导体以及金属掺杂氧化物半导体。本文在表 1 中统计了各类 MOS 基乙醇传感器关于检测浓度、工作温度、响应值等气敏参数并详细分析了具有代表意义的不同基乙醇传感器亮点。

2.1 氧化锌(ZnO)基乙醇传感器

氧化锌(ZnO)是一种常见的、理化性质稳定的 N 型半导体,其具有较宽的能隙(3.65 eV)、优异的电/化学性质、出色的气敏特性以及稳定的六方对称性结构。未经掺杂的 ZnO 内部载流子迁移率可通过改变合成温度、湿度、方式,达到 120 ~ 440 $cm^2 \cdot V/s$。因此,ZnO 基传感器被广泛用于检测各类有毒有害气体。

水热法(Hydrothermal)是制备 ZnO 基乙醇传感器最为普遍的方法,通过控制反应物类别、前驱体溶液酸碱度、水热反应时长以及退火时长获得形貌不一的 ZnO 敏感材料,如:纳米片状、纳米线状、空心核-壳状等。Wang 等人[42]通过控制水热反应条件及退火温度合成了具有丰富晶界的分等级 ZnO 纳米网状结构,相较于纳米片结构,分等级 ZnO 纳米网传感器对 100 ppm 乙醇具有 398 的高灵敏度响应和 4 s 的快速响应时间;除此之外,他们还提出了晶界传感增强效应模型(The Model of Sensing Enhancement Effect of Grain Boundary),认为网状结构可提供更多的氧空位以及吸附大量的氧分子使得电子耗尽层增大从而改善传感器灵敏度并通过实验验证了该理论模型。Li 等人[41]运用水热法制备出以多孔纳米片 ZnO 为敏感材料且不受外界湿度影响的乙醇传感器,其在 307 ℃下对 200 ppm 乙醇气体的响应值为 212,对该浓度乙醇气体的响应/恢复时间分别为 8 s 和 7 s;在选择性测试中,其对乙醇的敏感程度远高于氨气、甲醛、氯仿、甲醇、甲苯,大约为这些气体的 7 ~ 45 倍,具有良好的乙醇选择性;通过对敏感机理和密度泛函理论(Density Functional Theory,DFT)模拟的研究,解释了乙醇与多孔 ZnO 基传感器间的相互作用、传感器性能改善原因,为通过 ZnO 基材料的设计进一步提高乙醇传感性能提供了方案。

DFT 是一种研究多电子体系电子结构的方法,为解释气体传感器敏感机理提供了有效方式。Achmad 等人[111]研究了 Ag 掺杂对 ZnO 纳米片传感器探测乙醇气体灵敏度的影响并运用 B3LYP 杂化泛函方法探究乙醇气敏过程。基于 B3LYP 结果:未掺杂 ZnO 基传感器在 300 K 下对乙醇的响应为 6.2,而经 Ag 掺杂的 ZnO 基传感器的响应值显著上升至 72 且乙醇响应时间缩短,这是由于负载有 Ag 原子的 ZnO 表面对乙醇的吸附能从-6.1 kcal/mol 增加至-20.0 kcal/mol。Amea 等人[38]运用水热法制备的 4 wt% Au 掺杂 ZnO 显示出比 ZnO 基传感器高出 5 倍的响应,并且用 DFT 计算证实了实验结果。

溶剂热法(Solvothermal)是除水热法外另一种被广泛使用的低成本、易制备的传感器敏感材料制作工艺。Min 等人[40]提出了一种基于四种有机酸合成具有丰富表面缺陷 O 的 ZnO 纳米材料的溶剂热法。有机酸用作配体与 Zn^{2+} 形成络合物,在 ZnO 晶体形成过程中通过配位键的断裂产生更多的气体活性缺陷,暴露出更多易被乙醇分子吸附的(002)和(100)晶面。气敏测试结果显示,基于柠檬酸合成的 ZnO 表现出最佳的灵敏度(100 ppm—121.5)

且在 180 ℃的低工作温度下对乙醇具有优异的选择性。Baharuddin 等人[112]制备的氮掺杂 ZnO 基乙醇传感器可在 150 ℃下工作,并且将乙醇检测下限由 1 000 ppm 精确至 20 ppm。

2.2　二氧化锡(SnO_2)基乙醇传感器

二氧化锡(SnO_2)是晶格结构为正六面体形,带隙宽度在 3.5 ~4.0 eV 之间的 N 型半导体。通过不同制备工艺或条件制备所得的 SnO_2基传感器在检测不同浓度、不同成分、不同类型的气体方面皆有良好的敏感性能,以至于 SnO_2基传感器在气体传感器中占比近 40%。

最佳工作温度是衡量气体传感器功耗的重要指标,通常工作温度越低代表维持传感器最佳工作状态所需能耗越少。在较低工作温度下,传感器受温度影响降低,使用寿命增长。目前市面上在售乙醇传感器大多工作在 250 ℃及以上,而本节中乙醇传感器的最佳工作温度普遍在室温至 250 ℃区间,与国内节能减排战略目标相契合。Niavol 等人[36]运用水热法制备出还原性氧化石墨烯(rGO)与 SnO_2纳米颗粒相复合的乙醇传感器,与未负载 rGO 的 SnO_2基传感器相比,该传感器最佳工作温度降低了 80 ℃,对乙醇有极短的响应时间(1 s)且具有极佳的稳定性。通过表征设备发现:rGO/SnO_2纳米颗粒比表面积高达 128.52 m^2/g、孔体积为 0.14 cm^3/g、孔径平均为 4.39 nm,此项纳米颗粒数据表明 rGO/SnO_2基传感器在检测乙醇气体时可以与附着在其表面上更多的游离氧发生电荷交换过程,对降低传感器功耗、提升响应速度、改善稳定性起到决定性作用。Wang 等人[30]采取引入 Mo 元素方式降低了 SnO_2的结晶度,产生氧空位并增加电子浓度。在 220 ℃下,使富含氧空位的 5 mol% Mo 掺杂 SnO_2纳米管传感器对 100 ppm 乙醇的响应为 46.8,且在长达 90 天的测试期间保持着良好的稳定性。Wang 团队[29]还系统研究了 Tb 掺杂浓度对 SnO_2传感性能的影响,并证实与其他 Tb 掺杂剂浓度相比,7 mol% Tb 掺杂 SnO_2基传感器对乙醇气体具有最佳传感性能。在气敏检测过程中,该团队发现最佳工作温度随 Tb 掺杂浓度的增加呈降低趋势并进行了相关理论分析,认为 Tb 掺杂可以增加氧空位的数量,为乙醇分子附着到敏感材料表面提供更多的活性位点,从而有效促进乙醇气体在 SnO_2表面的吸附和反应,改善气敏性能。

由此可见,增大敏感材料比表面积、孔径对提供氧活性位点有极大关联,对改善传感器传感性能、功耗有决定性作用。经研究发现三维分等级结构、核-壳结构比纳米棒和纳米片这类低维结构拥有更大的比表面积、更高的孔隙率。Nd 等人[34]通过模拟蒸发诱导自组装过程,喷墨打印了可对 100 ppm 乙醇显示出 1 050 高响应值的孔径可调、高表面积-体积比、共连续介孔 SnO_2薄膜乙醇传感器。Xu 等人[23]采用静电纺丝技术制备 Pr 掺杂 SnO_2空心纳米管,其具备更大的气体分子接触表面,对改善乙醇传感性能起到重要作用。Feng 等人[28]通过利用锡基聚合物的直接分解制备了孔径可调(55 ~ 110 nm)的介孔球状 SnO_2基传感器,其孔尺寸约为 5.8 nm、比表面积介于 80.9 ~ 185.6 m^2/g,促使传感器在 250 ℃时对 50 ppm 乙醇的响应值为 18.9 且具有出色的选择性和稳定性。

2.3　其他 N 型 MOS 基乙醇传感器

氧化钒(V_2O_5)是一种极为稳定、环保、无害的 N 型半导体,禁带宽度为 2.3 eV,其晶体结构能为气体分子提供更多的吸附位点,可被应用于乙醇气体传感器。Tadeo 等人[99]报道了 V_2O_5薄膜在不同沉积温度下(350 ℃、400 ℃和 450 ℃)对乙醇、NO_2、CO 和 VOCs 的气敏性能,使用简单且易于重复的内置多用途气体传感装置进行气体传感检测,发现 350 ℃下在石英衬底上超声雾化的高致密性 V_2O_5薄膜传感器的乙醇气敏性能最佳。Shoorangiz 等人[103]通过控制水热反应时长制备了花状 V_2O_5基乙醇传感器并测试分析了不同反应时长下制得传感器的乙醇气敏性能。测试发现,在水热温度为 150 ℃、反应时间为 4 h 条件下制得的 V_2O_5基传感器在 175 ℃工作温度下对乙醇气体的响应值最高,并且表现出极佳的选择性和可重复性。作者认为花状晶体结构具有更大的比表面积供乙醇气体分子吸附,同时花状结构可使气体在晶体内部快速扩散,为改善传感器气敏性能提供了帮助。

氧化铟(In_2O_3)是一种重要的宽禁带(3.75 eV)N 型 MOS 敏感材料,其常见的晶体结构为立方体形和菱形两种。这些具有不同晶体结构的 In_2O_3晶体可通过不同制备工艺获得,如:水热法、溶剂热法、微波水热法(Microwave-Assisted Hydrothermal)、

化学气相沉积法(Chemical Vapor Deposition,CVD)等。Jin 等人[87]运用水热法制备出具有分等级结构的多孔 In_2O_3 纳米球,其具有均匀的尺寸、形状和高占比的氧空位含量(O_V:45.2%)。高占比氧空位含量的 In_2O_3 可吸附更多的游离氧并在晶粒间形成更宽的电子耗尽层,使 In_2O_3 接触乙醇气体时耗尽层变化量更大,促使这种多孔 In_2O_3 纳米球传感器对 200 ppm 乙醇的响应为 180,响应时间为 1 s 且工作温度较低(240 ℃)。Liang 等人[89]通过微波水热法合成了菱形(Rhombohedral)h-In_2O_3、立方形(Cubic)c-In_2O_3 以及菱形-立方混合形(Mix)m-In_2O_3 纳米颗粒。通过气敏性能比较发现 h-In_2O_3 比其他晶体结构具有更好的气敏特性,如:h-In_2O_3 基传感器对乙醇具有极佳的选择性(相较于 NH_3、CH_4、H_2、CO、CO_2 和 NO_2)、较低的乙醇检测下限(5 ppm)以及较好的稳定性(21 天)。这是由于 h-In_2O_3 具有优异的导电性、比表面积大(4.91 m^2/g)以及可供更多气体分子吸附的(104)晶面。

近期,氧化钨(WO_3)也常被用作乙醇传感器敏感材料,其具有复杂且灵活多变的晶体结构,是一种禁带宽度在 2.6~3.25 eV 之间的 N 型半导体。Spagnoli 等人[90]采用溶剂热法制备了可用于选择性乙醇传感的 WO_3 纳米片厚膜传感器,其不仅受环境湿度影响较小且在较低的工作温度(250 ℃)下对 50 ppm 乙醇响应值为 20.5。WO_3 虽被用于光催化、气体传感器、太阳能电池等场景,但受到氧空位数量、化学/热稳定性以及对部分气体敏感度较低等限制,WO_3 基气体传感器气敏性能可能有所影响。然而,单斜相(Monoclinic)$W_{18}O_{49}$ 因表面具有更多的氧空位可提升氧分子和待测气体分子的吸附活化能力而备受气体传感领域关注。Ou 等人[91]运用水热—光化学沉积法(Hydrothermal-Photodeposition)构建了具有优良气敏性能的 Pt/$W_{18}O_{49}$ 传感器,通过 DFT 计算了 Pt 纳米颗粒与 $W_{18}O_{49}$ 之间的界面机制效应,讨论了 Pt/$W_{18}O_{49}$ 和 $W_{18}O_{49}$ 传感器的吸附活化能,通过气相色谱仪对 Pt 掺杂前后的 $W_{18}O_{49}$ 传感器之间反应过程中消耗的乙醇量和产生的二氧化碳量进行了研究。经气敏机理研究发现:气敏性能被改善的主要原因在于 Pt 与 $W_{18}O_{49}$ 之间形成的欧姆接触可以有效提升电子迁移能力以及增强气体分子活性。

2.4 P 型 MOS 基乙醇传感器

在气体传感领域中,N 型半导体传感器对相同被测气体的响应值是 P 型半导体传感器响应值的平方倍[113],导致 N 型半导体传感器具有更大的市场占有率。然而 P 型半导体相较于 N 型半导体有着得天独厚的催化活性,使得 P 型半导体传感器可以有效检测有机挥发性气体且选择性更好。

氧化铜(CuO)是一种窄禁带宽度(1.2 eV)的 P 型半导体,其具有单斜相结构,晶格常数 a=4.683 Å,b=3.421 Å,c=5.129 Å,常被用作电池、薄膜晶体管、生物传感器和气体传感器。CuO 基气体传感器对乙醇、一氧化碳等还原性气体有很好的灵敏度,可准确监测气体浓度变化并做到实时响应。Ambardekar 等人[97]制备的 CuO 基乙醇传感器在 300 ℃下对 300 ppm 乙醇具有优异的气体响应,响应值为 844%,这可能是由于传感器具有较低的吸附活化能、较小的气体扩散直径等。Umar 等人[106]使用水热法制备出 CuO 空心微球传感器不仅对乙醇气体有极佳的灵敏度(100 ppm—13.2)和很好的选择性,并且具有较低的检测下限(25 ppm)。

氧化镍(NiO)是一种有着良好的电学和化学特性的 P 型传感器敏感材料。未经掺杂的 NiO 基气体传感器传感性能较弱,需要经过表面修饰和构建分等级结构来提高气体响应性能。例如,Shailja 等人[107]制备的 Ga 掺杂 NiO 纳米颗粒乙醇传感器相较于未掺杂的 NiO 传感器,3 at% Ga/NiO 基传感器在 250 ℃下对 50 ppm 乙醇表现出很高的响应值(25),响应/恢复时间为 8 s/13 s,且可检测到 10 ppm 乙醇气体。作者认为 NiO 晶粒尺寸小、表面缺陷浓度大、更大的比表面积以及较低的活化能对改善传感器乙醇气敏性能有积极作用。

2.5 复合 MOS 基乙醇传感器

复合金属氧化物半导体被看作是与单一 MOS 性能相比有着优异的物理、化学和机械性能的可替换气敏材料。一般来讲,复合气敏材料是在工艺制造环节由两种或多种不同导电类型半导体构建,从而形成异质结。在异质结内部,电子与空穴向着相反导电类型半导体路径迁移,直至费米能级实现平衡。该过程会使形成异质结的 N 型与 P 型 MOS 在二者接触面构建空穴积累层,继而推动气体分子在气敏材料表面的氧化还原反应进程达到优化气体传

感器气敏性能的目标。经过多年的广泛研究证明,复合金属氧化物半导体材料特性远超于传统的MOS 材料,其不仅可被用于气体传感器,还在生物传感器、湿度传感器[114]、光电探测器[115]、太阳能电池等领域发挥效用。在气体传感方面,制备复合MOS 基传感器的主要目的是在最佳温度下改善传感器的气敏特性。

目前,已有各种复合 MOS 的组合,如 Co_3O_4/NiO、MoS_2/TiO_2和 $FeVO_4$/ZnO 等用于乙醇气体检测。Yu 等人[55]采用原位沉淀法制备了半径为 0.8 ~ 1.4 μm 的 8 wt% CuO/$ZnSnO_3$空心微球,以该微球为敏感材料的气体传感器在较低的工作温度下(160 ℃)对 100 ppm 乙醇具有高气体响应值(131)。响应性能的提高可归因于 CuO 和 $ZnSnO_3$之间形成的 P-N 异质结。Zhao 等人[57]构建了由直径为 20 ~ 50 nm 的 CuO 纳米颗粒和直径为 30 ~ 50 nm 的 ZnO 纳米线复合的 P-N 异质结,制备了基于 CuO/ZnO P-N 结纳米线的气体传感器并比较了它们的气敏性能,发现通过 P-N 结复合结构有效地提高了 ZnO 纳米线传感器的乙醇传感性能。Zhang 等人[74]采用水热法制备的 Sn、Cu 摩尔比为 1∶1 的 SnO_2/CuO 基气体传感器对乙醇气体具有优异的选择性,对 100 ppm 乙醇的响应值达到 8.0,响应/恢复时间分别为 4 s 和 10 s,且传感器的响应值与 50 ~ 300 ppm 的乙醇浓度具有良好的线性关系。Zhang 团队[82]还通过探究采用静电纺丝法制备的 Sn、Cu 摩尔比为 1∶1 的 SnO_2/CuO 纳米管基传感器乙醇气敏性能,印证了 P-N结构和 Sn、Cu 摩尔比例对传感器性能改善有重要影响。Wang 等人[79]制备了用于乙醇传感器的新型花椰菜形 Bi_2O_3/ZnO 敏感材料。Bi_2O_3/ZnO 基传感器在 175 ℃下具有 7 s 的短响应时间,检测范围从 1 ~ 500 ppm,这可能是 P-N 异质结以及 β-Bi_2O_3晶相能够显著提高乙醇传感性能。Yan 等人[59]通过溶剂热法制备了 ZnO/In_2O_3多孔纳米片乙醇传感器,该传感器在长时间自然湿度下表现出优异的乙醇传感性能,可检测 0.1 ppm 乙醇气体,在老化 10 个月后,该装置仍可对醉酒受试者表现出快速反应(~3 s)。这主要是因为多孔纳米片结构具有高气体可及性、片状结构厚度小于两倍德拜长度(当晶粒尺寸小于材料两倍德拜长度时,传感器气敏性能会大幅提升[116])以及大量的活性位点和异质结构。该研究满足了现实世界中可重复且可靠的优越乙醇传感性能的测试。另外,紫外光也可促使具有 P-N 异质结构的乙醇传感器气敏性能改善。Li 等人[67]通过两步反应和退火合成了三维 SnO_2/ZnO 气凝胶并发现以气凝胶为敏感材料的气体传感器在紫外光激发下可以检测到 0.01 ppm 的超低浓度乙醇。这可能是因为:(1)充分的介孔结构增加了活性位点,利于乙醇气体分子流动,提高了紫外光的利用率;(2)气凝胶吸收丰富的紫外光能量,产生更多的光生电子;(3)协调后的带隙结构可提供更多的光生电子,减小传感器在乙醇气氛中的电阻。Zhang 等人[73]采用静电纺丝法制备了多重 N-N 异质结构的多孔 ZnO/SnO_2/Zn_2SnO_4纳米纤维并提出了紫外光激发增强乙醇响应的传感机制;解释了传感器的乙醇气敏性能增强是由于异质结纳米纤维在紫外光照下,自身的光吸收和电荷分离速率得到提高。

表 1　MOS 乙醇传感器性能比较

Table 1 Comparison of MOS ethanol sensor performance

制备方法 Method	传感器 Sensor	响应值 Response	工作温度 T (℃)	乙醇浓度 Ethanol Conc. (ppm)	响应时间 Res. Time (s)	回复时间 Rec. Time (s)	Ref.
Electrospinning	Pr/SnO_2	35.6[a]	200	100	12	8	[23]
Hydrothermal	SnO/rGO	4.6[a]	170	5	20	88	[24]
Hydrothermal	Sm/SnO_2	138.9[a]	160	50	NA	NA	[25]
Solvothermal	SnO_2	3.18%[c]	84	1 000	13	4	[26]
Hydrothermal	SnO_2	5.3[a]	200	20	0.75	50	[27]
Self-Template Strategy	SnO_2	18.9[a]	250	50	4	44	[28]

Electrospinning	Tb/SnO_2	53.6[a]	200	100	3.1	48	[29]
Electrospinning	Mo/SnO_2	46.8[a]	220	100	7	103	[30]
Hydrothermal	$Au-SnO_2$	213[a]	250	100	NA	NA	[31]
Thermal Decomposition	Pd/SnO_2	NA	RT	40	107	378	[32]
Sol-Gel	SnO_2	7.21[a]	120	40	47	272	[33]
Inkjet Printing	SnO_2	1050[a]	350	100	9	129	[34]
Pyrolysis	Ag/SnO_2	157[a]	250	10	NA	NA	[35]
Hydrothermal	SnO_2/rGO	16.77[a]	130	600	1	NA	[36]
NA	CNTs-ZnO/PS	2[a]	RT	500	18	29	[37]
Hydrothermal	Au/ZnO	525[a]	400	100	3	NA	[38]
Hydrothermal	ZnO	212[a]	307	200	8	7	[39]
Solvothermal	ZnO	121.5[a]	180	100	11	216	[40]
Hydrothermal	ZnO/ZnS	114.2[a]	325	100	3	8	[41]
Hydrothermal	ZnO	398[a]	280	100	4	63	[42]
NA	ZnO	89%[c]	300	60	60	NA	[43]
RF	ZnO/Au/ZnO	15[a]	12.17 Mw	100	NA	NA	[44]
Hydrothermal	Au/ZnO	15[a]	200	50	NA	NA	[45]
Sol-Gel	ZnO/Co	19[a]	235	2 500	10	52	[46]
Electrospinning	Au/ZnO	151.86[a]	200	50	NA	NA	[47]
Hydrothermal	Ag/ZnO	90%[c]	RT	1 000	NA	NA	[48]
Hydrothermal	ZnO/ZnS	55.34[a]	260	100	NA	NA	[49]
CVD	ZnO	9.2[a]	200	20	490±27	566±17	[50]
NA	Au/ZnO	37.74[a]	250	100	19	9	[51]
Hydrothermal	Pd/neck-connected-ZnO	311[a]	250	50	94	85	[52]
Electrospinning+Hydrothermal +Photo-Assisted Deposition	Au/ZnO	323[a]	220	1 000	NA	NA	[53]
Hydrothermal	Co/ZnO	279.8[a]	348	100	5	18	[54]
In-Situ Precipitation	$CuO/ZnSnO_3$	131[a]	160	100	13	8	[55]
Electrospinning	Au/SnO_2/ZnO	36.2[a]	300	100	2	59	[56]
Solvothermal	CuO/ZnO	28[a]	300	100	2	72	[57]
Hydrothermal	$g-C_3N_4-Zn_2SnO_4$	45[a]	290	100	15	23	[58]
Solvothermal	$ZnO-In_2O_3$	3.3[b]	320	3	3	8	[59]
Hydrothermal	MoO_2-Ni-Graphene	54[a]	RT	100	NA	NA	[60]

NA	$Au-SnO_2-In_2O_3$	37/53[b]	350	200	5/5	90/33	[61]
NA	$Pt/TiO_2/SnO_2$	7.59[a]	130	1	NA	NA	[62]
Hydrothermal	graphene/ZnO	26[a]	125	1	NA	NA	[63]
Sol-EPD	Ag-ITO	70%[c]	130	100	45	40	[64]
Hydrothermal+In-Situ Growth	Co_3O_4/NiO	4.26[b]	250	100	NA	NA	[65]
Hydrothermal	PdO_x/Co_3O_4	19.6[b]	130	50	43	14	[66]
Hydrothermal	SnO_2-ZnO	1.44[a]	300, UV	0.01	2	37	[67]
Hydrothermal	$ZnO/In_2O_3/ZnO$	453.2[a]	200	100	NA	NA	[68]
NA	ZnO/Co_3O_4	34.9[a]	300	10	57	235	[69]
Electrospinning	Co_3O_4 - ZnO	101.5[a]	275	100	NA	NA	[70]
NA	MoS_2/TiO_2	100%[d]	300	500	NA	NA	[71]
Hydrothermal	$Ba_{0.9}La_{0.1}FeO_3/SnO_2$	143[a]	250	1	NA	NA	[72]
Electrospinning	$ZnO-SnO_2-Zn_2SnO_4$	121[a]	130, UV	200	NA	NA	[73]
Hydrothermal	SnO_2-CuO	8[a]	320	100	4	10	[74]
Electrospinning	Fe_2O_3/Co_3O_4	37.8[b]	160	100	NA	NA	[75]
Hydrothermal	$W_{18}O_{49}$/Graphene	4.54[a]	340	20	1	5	[76]
Hydrothermal	MoS_2/TiO_2	62%[d]	350	100	52	155	[77]
Solution Processing	NiO-doped apple pectin film	16 100%[d]	250	10	1.379	1.057	[78]
Hydrothermal	Bi_2O_3/ZnO	21.6[a]	175	100	7	8	[79]
Solvothermal	Bi-doped rGO/Co_3O_4	150[b]	120	100	89	75	[80]
Hydrothermal	$FeVO_4/ZnO$	42[a]	300	400	26	79	[81]
Electrospinning	SnO_2/CuO	8.8[a]	340	250	6	10	[82]
RF	Au/In-Ga-Zn-O	27.9[a]	250	100	102	68	[83]
Co-Precipitation	Co_3O_4-ZnO/NC	49.2[b]	400	50	NA	NA	[84]
Hydrothermal	a-MnO_2	30.6[a]	300	200	30	40	[85]
Solvothermal	Co/WO_3	2.339[a]	250	20	NA	NA	[86]
Hydrothermal	In_2O_3	180[a]	240	200	1	93	[87]
CVD	Sb/In_2O_3	41.3[a]	320	100	17	36	[88]
MicoHydrothermal	In_2O_3	43.1[a]	300	100	37.6	1 454.5	[89]
Solvothermal	WO_3	20.5[a]	250	50	NA	NA	[90]
Hydrothermal - Photodeposition	$Pt/W_{18}O_{49}$	59[a]	300	80	20	10	[91]
Electrospinning	Ru/WO_3	120[a]	200	100	1	18	[92]
Solvothermal	In_2O_3	250[a]	250	50	16	14	[93]

Sol-Gel	N/In_2O_3	313[a]	250	300	1	480	[94]
Hydrothermal	WO_3	26.48[a]	160	100	1	30	[95]
Hydrothermal	CuO	2.8[b]	250	100	NA	NA	[96]
NA	CuO	844%[d]	300	300	NA	NA	[97]
Hydrothermal	α-Fe_2O_3	13.1[b]	400	100	3	108	[98]
NA	V_2O_5	81.7%[c]	280	200	17.6	39.7	[99]
Vapor-Liquid-Solid	α-Bi_2O_3	34.1[b]	350	40	NA	NA	[100]
Solvothermal	α-Fe_2O_3	35.15[a]	285	500	12	41	[101]
Hydrothermal	α-Fe_2O_3	26.05[a]	300	100	16	27	[102]
Hydrothermal	V_2O_5	50%[c]	175	20	NA	NA	[103]
Sol-Gel	α-Fe_2O_3	14.5%[d]	150	100	NA	NA	[104]
Electrophoretic Deposition	CuO	129%[d]	300	300	38	462	[105]
NA	CuO	13.2[b]	225	100	NA	NA	[106]
NA	Ga/NiO	25[b]	250	50	8	13	[107]
Hydrothermal	CuO	241%[d]	250	100	NA	NA	[108]
Co-Precipitation	Ag/α-Fe_2O_3	240%[d]	RT	20 mg/L	NA	NA	[109]
Hydrothermal	Ag/V_2O_5	22.5[a]	RT	500	13 (5 ppm)	7 (5 ppm)	[110]

注：a：(R_a/R_g)，b：(R_g/R_a)，c：($[R_a-R_g]/R_a*100\%$)，d：($[R_g-R_a]/R_g*100\%$)，NA：Not Available

本章节中，我们主要讨论和分析了用于乙醇气体传感器的各种金属氧化物半导体的特性、优点、局限和传感器性能。总结得出，无论是灵敏度亦或是功耗、选择性，SnO_2、ZnO 基乙醇传感器大多比其他 MOS 基乙醇传感器气敏性能优异。此外，提升乙醇传感器灵敏度、选择性，降低传感器功耗、响应/恢复时间等性能参数，可从掺杂金属元素的使用以及制备晶粒尺寸较小、比表面积大、孔隙率高的分等级结构敏感材料入手。与此同时，构建复合金属氧化物半导体异质结对改善乙醇传感器气敏性能有着积极作用。

3 结论

本篇综述总结了以不同制造工艺制备的电阻型 MOS 基乙醇传感器的气敏性能。本项工作以分等级金属氧化物半导体纳米结构为中心，通过文献总结后发现，具备比表面积大、孔隙率高、表面反应活性强的分等级敏感材料，能够显著提升传感器对乙醇气体的传感性能。文中所综述材料大多为 ZnO、SnO_2、In_2O_3、WO_3、CuO 这类成本低、开采便捷、制备简易的无公害气敏材料，具有与各种制备方法兼容的特点。通过不同的制备工艺，如：水热法、溶剂热法、共沉淀法、化学气相沉积法等，调控晶体结构、晶粒尺寸形成分等级结构达到改善传感器气敏性能的目的。我们发现表面形貌、孔隙大小、晶粒尺寸等对传感器的气敏参数具有主要影响作用，金属掺杂(Au、Ag、Pd 等)、异质结构建对改善传感器气敏特性具有重要意义。现如今，学界一直专注于 MOS 纳米结构的创新合成方法来改善传感器气敏特性。提升灵敏度、选择性、稳定性，降低工作温度、检测下限俨然成为增强气体传感器敏感性能的主要关注点，目的是为可大规模生产、高度可集成化高性能低功耗乙醇传感器作研发背景支撑。

参考文献：

[1] Seiyama T, Kagawa S. A New sDetector for Gaseous Components Using Semiconductive Thin Films [J]. Analytical

Chemistry, 1966, 38(8): 1502-1503.

[2]Nazemi H, Joseph A, Park J, et al. Advanced Micro- and Nano-Gas Sensor Technology: A Review [J]. Sensors, 2019, 19(6): 1285.

[3]Lou C, Yang C, Zheng W, et al. Atomic layer deposition of ZnO on SnO_2 nanospheres for enhanced formaldehyde detection [J]. Sensors and Actuators B Chemical, 2021, 329: 129218.

[4]Shuang Z A, Tq A, Jin L, et al. Design and sensing characteristics of ethanol fiber probe elaborated by ZnO nanosheets [J]. Journal of Physics and Chemistry of Solids, 2021, 162: 110495.

[5]Bartolomé J, Taeo M, Martínez-Casado R, et al. Ethanol gas sensing mechanisms of p-type NiO at room temperature [J]. Applied Surface Science, 2021, 579: 152134.

[6]Qiang H A, Wz A, Xw A, et al. Binder-free CuO nanoneedlearrays based tube-type sensor for H2S gas sensing [J]. Sensors and Actuators B: Chemical, 2020, 326: 128993.

[7]Duan G, Xu Z, Zhang H, et al. In situ synthesis of porous array films on a filament induced micro-gap electrode pair and their use as resistance-type gas sensors with enhanced performances [J]. Nanoscale, 2015, 7(34): 14264-14271.

[8]Pvt A, Lhma B, Nvd B, et al. Porous In_2O_3 nanorods fabricated by hydrothermal method for an effective CO gas sensor [J]. Materials Research Bulletin, 2020, 137: 111179.

[9]Ttla B, Dsk A, Jwy A, et al. Rapid synthesis of rhombohedral In_2O_3 nanoparticles via a microwave-assisted hydrothermal pathway and their application for conductometric ethanol sensing [J]. Sensors and Actuators B: Chemical, 2021, 346: 130578.

[10]Zhang X, Chen J, Wen M, et al. Solvothermal preparation of spindle hierarchical ZnO and its photocatalytic and gas sensing properties [J]. Physica B Condensed Matter, 2020, 602: 412545.

[11]Yang H, Lei Q, Zhao Z, et al. Electrospinning Encapsulation of Pd Nanoparticles into $\alpha-Fe_2O_3$ Nanofibers Windows Enhanced Acetone Sensing [J]. IEEE Sensors Journal, 2021, 21(14): 15944-15951.

[12]于　海. 锡氧化物分级微纳米结构材料的制备及其气敏特性的研究 [D]. 长春:吉林大学, 2017.

[13]Lee J H. Gas Sensors Using Hierarchical and Hollow Oxide Nanostructures: Overview [J]. Sensors and Actuators B Chemical, 2009, 140(1): 319-336.

[14]Yamazoe N. Toward innovations of gas sensor technology [J]. Sensors and Actuators B: Chemical, 2005, 108(1-2): 2-14.

[15]Cheng P F, Wang Y L, Wang Y, et al. C Investigation of doping effects of different noble metals for ethanol gas sensors based on mesoporous In_2O_3 [J]. Nanotechnology, 2021, 32(30): 305503.

[16]Yuan G, Zhang H, Cheng Y, et al. Hollow polyhedral Zn-Co_2O_4 superstructure as an ethanol gas sensor and sensing mechanism study using near ambient pressure XPS [J]. Journal of Materials Chemistry, C. materials for optical and electronic devices, 2021, 9(40): 14278-14285.

[17]Nejatinia S, Charvadeh S K, Khatibani A B. The effect of graphene and cobalt on ethanol sensing performance of ZnO based sensor prepared by sol-gel method [J]. Japanese journal of applied physics, 2022, 61(1): 017001.

[18]Barsan N, Koziej D, Weimar U. Metal oxide-based gas sensor research: How to? [J]. Sensors & Actuators B Chemical, 2007, 121(1): 18-35.

[19]Barsan N, Weimar U. Conduction Model of Metal Oxide Gas Sensors [J]. Journal of Electroceramics, 2001, 7(3): 143-167.

[20]Barsan N, Schweizer-Berberich M, Gpel W. Fundamental and Practical Aspects in the Design of Nanoscaled SnO_2 Gas Sensors: A Status Report [J]. Fresenius Journal of Analytical Chemistry, 1999, 365(4): 287-304.

[21]Franke M E, Koplin T J, Simon U. Metal and metal oxide nanoparticles in chemiresistors: does the nanoscale matter? [J]. Small, 2010, 2(1): 36-50.

[22]Kim H J, Lee J H. Highly sensitive and selective gas sensors using p-type oxide semiconductors: Overview [J]. Sensors & Actuators B Chemical, 2014, 192: 607-627.

[23]Xu X, Liu W, Wang S, et al. Design of high-sensitivity ethanol sensor based on Pr-doped SnO_2 hollow beaded tubular nanostructure [J]. Vacuum, 2021, 189: 110244.

[24]Gengzang D J, Chen W J, Chen Q, et al. Down to ppb level ethanol detection based on heterostructured SnO/rGO composites [J]. Materials Letters, 2021, 284: 128987.

[25]An D, Liu N, Li Y, et al. Synthesis of Sm doped SnO_2 nanoparticles and their ethanol gas traces detection [J]. Ceramics International, 2021, 47(18): 26501-26510.

[26]Tseng S F, Chen C W. Synthesis of nanograiny SnO_2 films on laser-patterned graphene/ceramic substrates for low-temperature ethanol gas sensors [J]. Ceramics International, 2021, 47(23): 33498-33508.

[27]Ge W, Zhang G, Wang P, et al. Highly selective detection of ethanol based on hierarchical three-dimensional

SnO_2: Combining experiment with first-principles calculation [J]. Sensors and Actuators A Physical, 2021, 331: 112994.

[28] Feng B, Feng Y, Qin J, et al. Self-template synthesis of spherical mesoporous tin dioxide from tin-polyphenol-formaldehyde polymers for conductometric ethanol gas sensing [J]. Sensors and Actuators B: Chemical, 2021, 341: 129965.

[29] Wang L, Ma S, Xu X, et al. Oxygen vacancy-based Tb-doped SnO_2 nanotubes as an ultra-sensitive sensor for ethanol detection [J]. Sensors and Actuators B Chemical, 2021, 344: 130111.

[30] Wang L, Ma S, Li J, et al. Mo-doped SnO_2 nanotubes sensor with abundant oxygen vacancies for ethanol detection [J]. Sensors and Actuators B: Chemical, 2021, 347: 130642.

[31] Cai Z, Goo E, Park S. Synthesis of tin dioxide (SnO_2) hollow nanospheres and its ethanol-sensing performance augmented by gold nanoparticle decoration [J]. Journal of Alloys and Compounds, 2021, 883: 160868.

[32] Vd A, Ls B, Ak B, et al. Pd doped SnO_2 based room temperature operable resistive sensor for the detection of ethanol vapors [J]. Materials Today: Proceedings, 2021, 46: 6437-6444.

[33] Sotelo J G, Bonilla-Ríos J, García-Escobar F, et al. Film Growth of Tetragonal SnO_2 on Glass Substrate by Dip-Coating Technique for Ethanol Sensing Applications [J]. Coatings, 2021, 11(3): 303.

[34] Nd A, Rp B, Amu B, et al. Ultra-high response ethanol sensors from fully-printed co-continuous and mesoporous tin oxide thin films [J]. Journal of Alloys and Compounds, 2021, 865: 158815.

[35] Xy A, Ls A, Jw A, et al. Metal organic frameworks derived SnO_2 microsphere doped Ag for monitoring low concentration ethanol [J]. Materials Science in Semiconductor Processing, 2021, 136: 106110.

[36] Niavol S S, Moghaddam H M. SnO_2 nanoparticles/reduced graphene oxide nanocomposite for fast ethanol vapor sensing at a low operating temperature with an excellent long-term stability [J]. Journal of Materials Science: Materials in Electronics, 2021, 32(5): 6550-6569.

[37] Hussein H T, Kareem M H, Hussein A M A. Synthesis and characterization of carbon nanotube doped with zinc oxide nanoparticles CNTs-ZnO/PS as ethanol gas sensor [J]. Optik, 2021, 248: 168107.

[38] Amea B, Em A, Nm A, et al. Experimental and density functional theory computational studies on highly sensitive ethanol gas sensor based on Au-decorated ZnO nanoparticles [J]. Thin Solid Films, 2021, 741: 139014.

[39] Qla B, Di C, Jma B, et al. Highly sensitive sensor based on ordered porous ZnO nanosheets for ethanol detecting application [J]. Sensors and Actuators B: Chemical, 2020, 326: 128952.

[40] Min X J, Qin W W, Zhang X, et al. An ultra-high sensitive ethanol sensor through amending surface-functionalized groups by novel acidic synthesis methods [J]. Sensors and Actuators B: Chemical, 2021, 347: 130654.

[41] Li Y, Song S, Zhang L B, et al. Fabrication of hollow porous ZnO@ZnS heterostructures via hydrothermal method and enhanced gas-sensing performance for ethanol [J]. Journal of Alloys and Compounds, 2021, 855: 157430.

[42] Wang B R, Wang R Z, Bai Y J, et al. Zinc oxide nanonets with hierarchical crystalline nodes: High-performance ethanol sensors enhanced by grain boundaries [J]. Journal of Alloys and Compounds, 2021, 877: 160277.

[43] By A, An B, Ob A, et al. Towards the development of a gas micro-sensor based on nano-structured zinc oxide thin film for ethanol gas detection [J]. Materials Today: Proceedings, 2022, 52: 89-94.

[44] Liu R, Xie D, Adedokun G, et al. A Low Power Bridge-Type Gas SensorWith Enhanced Sensitivity to Ethanol by Sandwiched ZnO/Au/ZnO Film Sputtered in O-2 Atmosphere [J]. IEEE sensors journal, 2021, 21(17): 18578-18587.

[45] Lei M, Gao M, Yang X, et al. Size-Controlled Au Nanoparticles Incorporating Mesoporous ZnO for Sensitive Ethanol Sensing [J]. ACS Applied Materials & Interfaces, 2021, 13(14): 51933-51944.

[46] Khatibani A, Shabankhah B. A Fabrication and ethanol sensing of sol-gel grown zinc oxide powder: the effect of cobalt and copper doping [J]. Applied Physics A-Materials Science & Processing, 2021, 127(5): 308.

[47] Li J P, Yang Y F, Wang Q, et al. Design of size-controlled Au nanoparticles loaded on the surface of ZnO for ethanol detection [J]. CrystEngComm, 2021, 23(4): 783-792.

[48] Zhang X, Wang W, Zhang D, et al. Self-powered ethanol gas sensor based on the piezoelectric Ag/ZnO nanowire arrays at room temperature [J]. Journal of Materials Science: Materials in Electronics, 2021, 32(6): 7739-7750.

[49] Zhang K, Lin Z. Highly sensitive ethanol sensor based on

zinc oxide-based nanomaterials with low power consumption [J]. Journal of Materials Science: Materials in Electronics, 2021, 32(13): 17395-17405.

[50] Navarrete E, Güell F, Martínez-Alanis P R, et al. Chemical Vapour Deposited ZnO Nanowires for Detecting Ethanol and NO_2 [J]. Journal of Alloys and Compounds, 2021, 890(1): 161923.

[51] Kang Y, Zhang L, Wang W, et al. Ethanol Sensing Properties and First Principles Study of Au Supported on Mesoporous ZnO Derived from Metal Organic Framework ZIF-8 [J]. Sensors, 2021, 21(13): 4352.

[52] Qi T J, Sun J, Yang X. Research on Ethanol Sensing Characteristics of Pd/Neck - Connected - ZnO Based Chemiresistive Sensors [J]. Chemistryselect, 2021, 6(19): 4797-4802.

[53] Vuong N M, Le H T, Phan T H, et al. Ultra Responsive and Highly Selective Ethanol Gas Sensor Based on Au Nanoparticles Embedded ZnO Hierarchical Structures [J]. Journal of The Electrochemical Society, 2021, 168(2): 027503.

[54] Wang X, Li H, Huang D, et al. Effect of Co-doping on the performance of nanosheet-like ZnO ethanol gas sensor [J]. Journal of Materials Science-Materials in Electronics, 2021, 32(22): 26529-26538.

[55] Yu S W, Jia X H, Yang J, et al. Highly sensitive ethanol gas sensor based on $CuO/ZnSnO_3$ heterojunction composites [J]. Materials Letters, 2021, 291: 129531.

[56] Li Y J, Zhang H M, Han S Q, et al. Novel porous orange-peel-like $Au/SnO_2/ZnO$ nanosheets with highly sensitive and selective performance to ethanol [J]. Materials Letters, 2021, 303: 130509.

[57] Zhao S, Shen Y, Hao F, et al. P-n junctions based on CuO-decorated ZnO nanowires for ethanol sensing application [J]. Applied Surface Science, 2021, 538(93): 148140.

[58] Akhtar A, Wen H, Chu X, et al. Synthesis of $g-C_3N_4-Zn_2SnO_4$ nanocomposites with enhanced sensing performance to ethanol vapor [J]. Synthetic Metals, 2021, 278: 116829.

[59] Yan W, Chen Y, Zeng X, et al. Ultrasensitive ethanol sensor based on segregated $ZnO-In_2O_3$ porous nanosheets [J]. Applied Surface Science, 2020, 535: 147697.

[60] Mehmood S, Zhao X, Bhopal M F, et al. MoO_2-Ni-graphene Ternary Nanocomposite for a High - Performance Room-Temperature Ethanol Gas Sensor [J]. Applied Surface Science, 2021, 554: 149595.

[61] Xu H Y, Akbari M K, Wei Z H, et al. Plasma-induced sub-10 nm $Au-SnO_2-In_2O_3$ heterostructures fabricated by atomic layer deposition for highly sensitive ethanol detection on ppm level [J]. Applied Surface Science, 2021, 563: 150400.

[62] Xin T, Hca B, Hwa B, et al. Optimal Pt mesoporous layer modified nanocomposite film with highly sensitive detection of ethanol at low temperature [J]. Applied Surface Science, 2021, 578: 151983.

[63] Rafiee Z, Roshan H, Sheikhi M H. Low concentration ethanol sensor based on graphene/ZnO nanowires [J]. Ceramics International, 2021, 47(4): 5311-5317.

[64] Afrouzmehr M, Yasrebi N, Sheikhi M H. Fabrication and characterization of Ag-Decorated indium - tin-oxidenanoparticle based ethanol sensors using an enhanced electrophoretic method [J]. Ceramics International, 2021, 47(21): 30504-30513.

[65] Guo S, Yang L, Liu C, et al. Hetero-epitaxy growth of cobalt oxide/nickel oxide nanowire arrays on alumina substrates for enhanced ethanol sensing characteristics [J]. Ceramics International, 2022, 48(3): 3849-3859.

[66] Ww A, Wei J B, Shuang Y A, et al. PdOx decorated Co_3O_4 nanosheets-assembled hollow microcages for enhanced ethanol sensing performance [J]. Sensors and Actuators B: Chemical, 2021, 333: 129583.

[67] Li H K, Yang Z Y, Ling W Y, et al. UV excited gas sensing SnO_2-ZnO aerogels to ppb-level ethanol detection [J]. Sensors and Actuators B: Chemical, 2021, 337: 129815.

[68] Wang S, Wang X, Qiao G, et al. Core-double shell ZnO @ In_2O_3 @ ZnO hollow microspheres for superior ethanol gas sensing [J]. Sensors and Actuators B: Chemical, 2021, 341: 130002.

[69] Tan L, Kim J Y, Lee J H, et al. Preparation of n-ZnO/p-Co_3O_4 heterojunctions from zeolitic imidazolate frameworks (ZIF-8/ZIF-67) for sensing low ethanol concentrations [J]. Sensors and Actuators B: Chemical, 2021, 348: 130684.

[70] Zhang J, Leng D, Li G, et al. Bimetallic - organic framework-derived Co_3O_4-ZnO heterojunction nanofibers: A new kind of emerging porous nanomaterial for enhanced ethanol sensing [J]. Sensors and Actuators B: Chemical, 2021, 349: 130732.

[71] Singh S, Sharma S. Temperature dependent selective detection of ethanol and methanol using MoS_2/TiO_2 composite [J]. Sensors and Actuators B: Chemical, 2022, 350:

130798.

[72] Suematsu K, Hiroyama Y, Watanabe K, et al. Amplifying the receptor function on $Ba_{0.9}La_{0.1}FeO_3-SnO_2$ composite particle surface for high sensitivity toward ethanol gas sensing [J]. Sensors and Actuators B: Chemical, 2021, 354: 131256.

[73] Zhang Y, Xin X, Sun H, et al. Porous $ZnO-SnO_2-Zn_2SnO_4$ heterojunction nanofibers fabricated by electrospinning for enhanced ethanol sensing properties under UV irradiation [J]. Journal of Alloys and Compounds, 2020, 854: 157311.

[74] Zhang J, Ma S, Wang B, et al. Hydrothermal synthesis of SnO_2-CuO composite nanoparticles as a fast-response ethanol gas sensor [J]. Journal of Alloys and Compounds, 2021, 886: 161299.

[75] Chen X H, Liang R, Qin C, et al. Coaxial electrospinning Fe_2O_3 @ Co_3O_4 double-shelled nanotubes for enhanced ethanol sensing performance in a wide humidity range [J]. Journal of Alloys and Compounds, 2021, 891: 161868.

[76] Qiu Y, Wang Y, Song C. Facile synthesis of $W_{18}O_{49}$/Graphene nanocomposites for highly sensitive ethanol gas sensors [J]. Colloids and Surfaces A Physicochemical and Engineering Aspects, 2021, 616: 126300.

[77] Singh S, Raj S, Sharma S. Ethanol sensing using MoS_2/TiO_2 composite prepared via hydrothermal method [J]. Materials today: proceedings, 2021, 46: 6083-6086.

[78] Chang S J. High Response of Ethanol Gas Sensor Based on NiO-Doped Apple Pectin by the Solution Process [J]. Coatings, 2021, 11(9): 1073.

[79] Wang P, Wang S Z, Kang Y R, et al. Cauliflower-shaped Bi_2O_3-ZnO heterojunction with superior sensing performance towards ethanol [J]. Journal of Alloys and Compounds, 2021, 854: 157152.

[80] Cai S X, Song X Q, Chi Z T, et al. Rational design of Bi-doped rGO/Co_3O_4 nanohybrids for ethanol sensing [J]. Sensors and Actuators B: Chemical, 2021, 343: 130118.

[81] Ou Y C, Zhu R L, Peng J H, et al. Formation of $FeVO_4$/ZnO n-n heterojunction with enhanced sensing properties for ethanol [J]. Applied Nanoscience, 2021.

[82] Zhang J, Ma S, Wang B, et al. Preparation of composite SnO_2/CuO nanotubes by electrospinning and excellent gas selectivity to ethanol [J]. Sensors and Actuators A Physical, 2021, 332: 113090.

[83] Peng R Y, Liu W C. Study of a High-Performance Chemoresistive Ethanol Gas Sensor Synthesized With Au Nanoparticles and an Amorphous IGZO Thin Film [J]. IEEE Transactions on Electron Devices, 2021, 68(2): 753-760.

[84] Zhang X, Xu Y, Wei F, et al. Synthesis of Porous Co_3O_4-ZnO and its Performance for Sensitive Ethanol Detection [C]. //16th IEEE International Conference on Nano/Micro Engineered and Molecular Systems (IEEE-NEMS), 2021, 1436-1440.

[85] Umar A, Ibrahim A A, Kumar R, et al. Gas sensor device for high-performance ethanol sensing using alpha-MnO_2 nanoparticles [J]. Materials Letters, 2021, 286: 129232.

[86] Lim J C, Jin C, Kim H S, et al. Synthesis, morphology, characterisation, and ethanol gas sensing of hierarchical flower-like Co-doped WO_3 nanoplates by solvothermal route [J]. Ceramics International, 2021, 47(15): 20956-20964.

[87] Jin X, Li Y, Zhang B, et al. Temperature-dependent dual selectivity of hierarchical porous In_2O_3 nanospheres for sensing ethanol and TEA [J]. Sensors and Actuators B Chemical, 2020, 330: 129271.

[88] Li X, Liu Y, Cheng P, et al. High-performance ethanol sensor of wrinkled microspheres by spray pyrolysis [J]. Sensors and Actuators B: Chemical, 2021, 344: 130309.

[89] Liang T T, Kim D S, Yu Y T, et al. Rapid synthesis of rhombohedral In_2O_3 nanoparticles via a microwave-assisted hydrothermal pathway and their application for conductometric ethanol sensing [J]. Sensors and Actuators B: Chemical, 2021, 346: 130578.

[90] Spagnoli E, Krik S, Guidi V, et al. Development and characterization of WO_3 nanoflakes for selective ethanol sensing [J]. Sensors and Actuators B: Chemical, 2021, 347: 30593-30593.

[91] Ou Y, Zhu G, Zhang W, et al. Achieving rapid response and high sensitivity in ethanol gas sensing using a Pt/$W_{18}O_{49}$ ohmic contact via modulating the adsorption and activation properties: Theoretical and experimental insights [J]. Sensors and Actuators B: Chemical, 2021, 347: 130601.

[92] Li J J, Ding Q L, Mo X C, et al. A highly stable and sensitive ethanol sensor based on Ru-decorated 1D WO_3 nanowires [J]. RSC Advances, 2021, 11(6): 39130-39141.

[93] Shen C, Xu N, Guan R F, et al. Highly sensitive ethanol gas sensor based on In_2O_3 spheres [J]. Ionics, 2021, 27(8): 3647-3653.

[94] Shihabudeen P K, Chaudhuri A R. Ethanol sensing properties of nitrogen doped-In_2O_3 thin films [J]. Journal of

Materials Researches, 2021, 36 (7): 1561-1572.

[95] Xiao J K, Che Y H, Song C W, et al. Synthesis of WO_3 Nanorods and Their Excellent Ethanol Gas-Sensing Performance [J]. Materials Research-Ibero-American Journal of Materials, 2021, 24(3): e20200434.

[96] Umar A, Ibrahim A A, Nakate U T, et al. Fabrication and characterization of CuO nanoplates based sensor device for ethanol gas sensing application [J]. ChemicalPhysics Letters, 2021, 763: 138204.

[97] Ambardekar V, Bhowmick T, Bandyopadhyay P P, et al. Ethanol and acetone sensing properties of plasma sprayed copper oxide coating [J]. The journal of physics and chemistry of solids, 2021, 160: 10333-10333.

[98] Umar A, Ibrahim A A, Kumar R, et al. Cubic shaped hematite (alpha-Fe_2O_3) micro-structures composed of stacked nanosheets for rapid ethanol sensor application [J]. Sensors and Actuators B Chemical, 2020, 326: 128851.

[99] Tadeo I J, Parasuraman R, Umarji A M. Highly sensitive and selective ultrasonically nebulized V_2O_5 thin films towards ethanol and NO_2 gas detection [J]. Sensors and Actuators B: Chemical, 2021, 337: 129811.

[100] Moumen A, Zappa D, Poli N, et al. Catalyst-Assisted vapor liquid solid growth of alpha-Bi_2O_3 nanowires for acetone and ethanol detection [J]. Sensors and Actuators B Chemical, 2021, 346: 130432.

[101] Zhang M G, Lu M Y, Cheng L F, et al. Quasi-cubic hematite with exposed high-energy facets for ethanol gas detection [J]. Journal of Alloys and Compounds, 2021, 873: 159667.

[102] Xiong H J, Fu J N, Li J Y, et al. Strain-regulated sensing properties of alpha-Fe_2O_3 nano-cylinders with atomic carbon layers for ethanol detection [J]. Journal of Materials Sciences & Technology, 2021, 68: 132-139.

[103] Shoorangiz M, Shariatifard L, Mirzaei A, et al. Hydrothermally synthesized flower-like vanadium oxide nanostructures for ethanol sensing studies [J]. Materials Science in semiconductor processing, 2021, 137: 106241.

[104] Shoorangiz M, Shariatifard L, Roshan H, et al. Selective ethanol sensor based on alpha-Fe_2O_3 nanoparticles [J]. Inorganic Chemistry Communications, 2021, 133: 108961.

[105] Bandyopadhyay A, Mandal K, Ambardekar V, et al. Electrophoretic deposition of CuO particulate thick film for ethanol sensing [J]. Journal of Materials Science: Material Electronics, 2021, 32(13): 17324-17335.

[106] Umar A, Ibrahim A A, Ammar H Y, et al. Urchin like CuO hollow microspheres for selective high response ethanol sensor application: Experimental and theoretical studies [J]. Ceramics International, 2021, 47(9): 12084-12095.

[107] Shailja, Singh K J, Singh R C. Highly sensitive and selective ethanol gas sensor based on Ga-doped NiOnanoparticles [J]. Journal of Materials Science: Materials in Electronics, 2021, 32(8): 11274-11290.

[108] Umar A, Ibrahim A A, Baskoutas S, et al. Selective ethanol gas sensing performance of flower-shaped CuO composed of thin nanoplates [J]. Journal of Materials Science: Materials in Electronics, 2021, 32(14): 18565-18579.

[109] Garciaosorio D, Hidalgofalla P, Peres H, et al. Silver Enhances Hematite Nanoparticles Based Ethanol Sensor Response and Selectivity at Room Temperature [J]. Sensors, 2021, 21(2): 440-440.

[110] Shah A H, Chen W, Ahmad F, et al. Significant SRS sensing behavior of hydrothermally silver decorated sandwiched-like vanadia (Ag-V_2O_5) nanosheets toward ethanol [J]. Applied Physics A-Materials Science & Processing, 2021, 127(6): 477.

[111] Achmad M H, Sarraf A, Bokov D O, et al. A DFT study on the Ag-decorated ZnO graphene-like nanosheet as a chemical sensor for ethanol: Explaining the experimental observations [J]. Inorganic Chemistry Communications, 2021, 133(48): 108892.

[112] Baharuddin A A, Ang B C, Wong Y H, et al. Improvement of N-ZnO chemiresistive gas sensor toward lower detection limit of acetone and ethanol at low operating temperature [J]. Materials Letters, 2021, 303: 130562.

[113] Hubner M, Simion C E, Weimar U, et al. Influence of humidity on CO sensing with p-type CuO thick film gas sensors [J]. Sensors & Actuators B Chemical, 2011, 153(2): 347-353.

[114] 丁书聪, 黄宜明, 王　晓, 等. 湿度传感元件制备,封装及检测电路设计的研究进展 [J]. 电子与封装, 2021, 21(1): 24-32.

[115] 徐春燕, 南海燕, 肖少庆, 等. 基于二维半导体材料光电器件的研究进展 [J]. 电子与封装, 2021, 21(3): 67-81.

[116] Dey A. Semiconductor metal oxide gas sensors: A review [J]. Materials Science and Engineering B-Advanced Functional Solid-State Materials, 2018, 229: 206-217.